Microbial exposure drives polyclonal expansion of innate γδ T cells immediately after birth

Sarina Ravens[a,b,1,2], Alina S. Fichtner[a,1], Maike Willers[c], Dennis Torkornoo[a], Sabine Pirr[c], Jennifer Schöning[c], Malte Deseke[a], Inga Sandrock[a], Anja Bubke[a], Anneke Wilharm[a], Daniel Dodoo, Beverly Egyir[d], Katie L. Flanagan[e,f,g,h], Lars Steinbrück[i], Paul Dickinson[j,k], Peter Ghazal[k], Bright Adu[d], Dorothee Viemann[c,b,l,1], and Immo Prinz[a,b,1]

[a]Institute of Immunology, Hannover Medical School, 30625 Hannover, Germany; [b]Cluster of Excellence RESIST – Resolving Infection Susceptibility (EXC 2155), Hannover Medical School, 30625 Hannover, Germany; [c]Department of Pediatric Pneumology, Allergology and Neonatology, Hannover Medical School, 30625 Hannover, Germany; [d]Noguchi Memorial Institute for Medical Research, College of Health Sciences, University of Ghana, Legon, Ghana; [e]Vaccines and Immunity Theme, Medical Research Council Unit, Fajara, The Gambia; [f]School of Medicine, University of Tasmania, Launceston, TAS 7250, Australia; [g]School of Health & Biomedical Science, RMIT University, Melbourne, VIC 3083, Australia; [h]Department of Immunology and Pathology, Monash University, Melbourne, VIC 3004, Australia; [i]Institute of Virology, Hannover Medical School, 30625 Hannover, Germany; [j]Centre for Genomic and Experimental Medicine, Institute of Genetics and Molecular Medicine, University of Edinburgh, Edinburgh EH16 4SB, United Kingdom; [k]Division of Infection and Pathway Medicine, University of Edinburgh, Edinburgh EH16 4SB, United Kingdom; and [l]PRIMAL (priming immunity at the beginning of life) Consortium, Germany

Edited by Rebecca L. O'Brien, National Jewish Health, Denver, CO, and accepted by Editorial Board Member Philippa Marrack June 17, 2020 (received for review January 8, 2020)

Starting at birth, the immune system of newborns and children encounters and is influenced by environmental challenges. It is still not completely understood how γδ T cells emerge and adapt during early life. Studying the composition of T cell receptors (TCRs) using next-generation sequencing (NGS) in neonates, infants, and children can provide valuable insights into the adaptation of T cell subsets. To investigate how neonatal γδ T cell repertoires are shaped by microbial exposure after birth, we monitored the γ-chain (*TRG*) and δ-chain (*TRD*) repertoires of peripheral blood T cells in newborns, infants, and young children from Europe and sub-Saharan Africa. We identified a set of *TRG* and *TRD* sequences that were shared by all children from Europe and Africa. These were primarily public clones, characterized by simple rearrangements of Vγ9 and Vδ2 chains with low junctional diversity and usage of non-*TRDJ1* gene segments, reminiscent of early ontogenetic subsets of γδ T cells. Further profiling revealed that these innate, public Vγ9Vδ2$^+$ T cells underwent an immediate TCR-driven polyclonal proliferation within the first 4 wk of life. In contrast, γδ T cells using Vδ1$^+$ and Vδ3$^+$ *TRD* rearrangements did not significantly expand after birth. However, different environmental cues may lead to the observed increase of Vδ1$^+$ and Vδ3$^+$ *TRD* sequences in the majority of African children. In summary, we show how dynamic γδ TCR repertoires develop directly after birth and present important differences among γδ T cell subsets.

TRG and TRD repertoires | neonatal γδ T cells | postnatal TCR repertoire focusing | Vγ9Vδ2 | non-Vγ9Vδ2

The composition and function of the immune system differs among newborns, children, and adults. Immune cells of newborns are disposed for Th2-like responses and/or immune tolerance (1, 2). Neonatal immunity is further characterized by little immunological memory and relies on responses of the innate branch of the immune system (1, 3). After birth, neonates are suddenly exposed to various environmental cues and a high variety of new antigens that challenge their immune system. One subpopulation of T lymphocytes, γδ T cells, could be an important contributor to early neonatal protection because they start to develop around gestational week 8 and show a high functional responsiveness in utero and in newborns (4–11). In contrast, adult γδ T cells are phenotypically distinct from neonatal γδ T cells both in T cell receptor (TCR) repertoire composition and innate- and adaptive-like functions (12, 13). In adults, γδ T cells have been assigned pleiotropic roles such as mediating tissue surveillance, tumor immunity, and immune responses against various pathogens, including *Mycobacterium tuberculosis*, *Cytomegalovirus* (CMV), or *Plasmodium falciparum* (12, 14).

γδ T cells express TCRs composed of individually rearranged γ-chains (*TRG*) and δ-chains (*TRD*), whereby random recombination of different variable (V)-, diversity (D)-, and joining (J)-gene elements creates a high TCR repertoire diversity (15). A number of studies have described γδ TCR repertoires based on "public and private" characteristics. According to this denomination, public repertoires indicate that TCR sequences are shared among many individuals and private repertoires are inherently different in each person. Based on their TCR's V-gene expression, ontogeny, and functionality, human γδ T cells can be grouped into either Vγ9Vδ2$^+$ or non-Vγ9Vδ2$^+$ T cells (16).

Vγ9Vδ2$^+$ T cells are the main γδ T cell population in second trimester thymus (7), but are rarely detected in pediatric thymi. As a matter of fact, neonatal Vγ9Vδ2$^+$ T cells are intrinsically primed to produce IFN-γ, IL-17, and granzymes proposing a unique effector role in neonatal immunity (7, 9, 10). With regard

Significance

T cell receptors (TCRs) on the surface of T cells mediate recognition of antigen. Since each new T cell carries an individual clonal TCR, monitoring of TCR repertoires reflects how T cells react and proliferate in response to environmental cues in the developing immune system of neonates and children. γδ T cells appear early during ontogeny and are important for immune surveillance. Here, we longitudinally analyze γδ T cells in neonates and show an immediate polyclonal expansion of phosphoantigen-reactive Vγ9Vδ2$^+$ T cells after birth. We also observed differences in γδ TCR repertoires of children from Europe and Africa. Our study highlights the importance of γδ T cells in the neonatal immune system and their prompt expansion directly after birth.

Author contributions: S.R., A.S.F., D.V., and I.P. designed research; S.R., A.S.F., M.W., D.T., J.S., M.D., I.S., A.B., and A.W. performed research; S.P., D.D., B.E., K.L.F., L.S., P.D., P.G., B.A., and D.V. contributed new reagents/analytic tools; S.R. and A.S.F. analyzed data; and S.R., A.S.F., and I.P. wrote the paper.

The authors declare no competing interest.

This article is a PNAS Direct Submission. R.L.O. is a guest editor invited by the Editorial Board.

Data deposition: FASTQ files of *TRG* and *TRD* sequences are deposited and available under the SRA accession code PRJNA592548.

[1]S.R., A.S.F., D.V., and I.P. contributed equally to this work.

[2]To whom correspondence may be addressed. Email: ravens.sarina@mh-hannover.de.

This article contains supporting information online at https://www.pnas.org/lookup/suppl/doi:10.1073/pnas.1922588117/-/DCSupplemental.

First published July 20, 2020.

to their immunological surveillance function, Vγ9Vδ2$^+$ TCRs interact with butyrophilin (BTN) molecules to sense prenyl pyrophosphate metabolites, called phosphoantigens (pAgs), in infected, stressed, or transformed cells (17–22). Those nonpeptide antigens are produced by many bacteria and parasites, including *M. tuberculosis*, *Escherichia coli*, or *Salmonella* and are highly potent activators of neonatal and adult Vγ9Vδ2$^+$ T cells (20, 23–25). After birth, bacteria of the developing skin and/or gut microbiota might be potent sources of pAgs that further shape, stimulate, and/or maintain the Vγ9Vδ2$^+$ T cell compartment in neonates, infants, and children (26, 27). In line with this, Vγ9Vδ2$^+$ T cells were described to expand and mature in children to subsequently become the main γδ T cell subset in adult peripheral blood (27, 28). Independent of age, their TCRs express a Vγ9 chain that exclusively rearranges with the *TRGJP* joining element, show few or no N insertions (29–31), and contain conserved regions that are important for ligand interaction (32–35). These invariant Vγ9JP$^+$ *TRG* sequences can be found in every individual and are considered public Vγ9JP$^+$ T cell clones (30, 31, 36, 37).

All other γδ T cell subsets utilize *TRG* rearrangements that are not Vγ9JP$^+$ and the majority of these pair with Vδ1 chains, less frequently with Vδ2 or Vδ3 chains, and are called non-Vγ9Vδ2$^+$ T cells hereafter. Non-Vγ9Vδ2$^+$ T cells also include innate T cell subsets that arise during early fetal development and express invariant TCRs, but are usually the minor γδ T cell fraction during early fetal development (6). Interestingly, these early innate-like non-Vγ9Vδ2$^+$ T cells are intrinsically primed for effector functions and can mount anti-CMV responses in utero (6, 8). In the last trimester, non-Vγ9Vδ2$^+$ T cells become the major γδ T cell subset (38) and leave the pediatric thymus as naïve T cells (39). These cells have an extremely high TCR repertoire diversity, express TCR sequences that are not shared among individual subjects, and are therefore described as private TCR repertoires (40, 41). In contrast to innate-like pAg-sensing Vγ9Vδ2$^+$ T cells, the TCR of non-Vγ9Vδ2$^+$ T cells may recognize a variety of ligands that range from MHC-like molecules to stress-induced cell surface molecules (42–44). In adult peripheral blood, non-Vγ9Vδ2$^+$ T cells (mainly Vδ1$^+$) are usually found at low frequencies, but some individuals display high Vδ1$^+$ T cell numbers that potentially stem from previous infectious diseases and may correlate with the CMV serology status (40, 45). Indeed, anti-CMV responses of Vδ1$^+$ T cells have been well described (8, 46–48) and next-generation sequencing (NGS) of γδ TCR repertoires revealed long-lasting expansion of CMV-induced Vδ1$^+$ T cell clones in adult patients (37). Therefore, an adaptive-like biology has been ascribed to peripheral non-Vγ9Vδ2$^+$ (mainly Vδ1$^+$) T cells (49). However, whether and how pathogens other than CMV shape the adaptation of peripheral blood non-Vγ9Vδ2$^+$ TCR repertoires remains elusive. Recent reviews speculated about different dynamics and environmental factors driving the postnatal adaptation of Vγ9Vδ2$^+$ and non-Vγ9Vδ2$^+$ T cells (29, 49, 50), yet data are lacking for neonatal and early childhood γδ T cells. To approach how peripheral blood γδ T cells evolve in the first weeks, months, and years of life, we monitored γδ TCR repertoires in four independent study populations of 1) preterm babies from Europe (Germany); 2) young children from Europe (Germany); 3) 9-mo-old infants from Africa (The Gambia); and 4) children from Africa (Ghana) and found evidence for a differential adaptation of Vγ9Vδ2$^+$ and non-Vγ9Vδ2$^+$ TCR repertoires after birth and during early childhood.

Results

Immediate Expansion of Vγ9Vδ2$^+$ T Cells after Birth. Canonical Vγ9Vδ2$^+$ T cells are a prominent subtype of human γδ T cells characterized by a semiinvariant phosphoantigen-reactive TCR that consists of Vγ9JP$^+$ rearrangements paired with Vδ2 chains. Their pAg reactivity was shown to depend on lysine residues that are encoded by the JP-gene segment (*TRGJP*) and is potentially influenced by hydrophobic amino acids (aa) at position 97 of the Vδ2 chain (L, I, and V) (32–35, 51). However, knowledge of how Vγ9Vδ2$^+$ TCR repertoires are shaped by pAg exposure after birth remains fragmentary. To understand how γδ T cells evolve in response to the strong microbial stimuli associated with birth, we tracked γδ T cells in the peripheral blood of European (E) preterm babies in the first 2 wk of life (w1-2 [E]) and as a followup after 3 to 5 wk (w3-5 [E]), and compared those to γδ T cell frequencies of healthy 1- to 3.5-y-old children (y1-3.5 [E]) (*SI Appendix*, Table S1). Flow cytometry (FACS) analysis of individual samples of preterm babies demonstrated that γδ T cells increased in frequencies and numbers within the first 2 wk after birth (Fig. 1 *A* and *B*) with γδ T cell frequencies at w3-5 reaching levels comparable to those in healthy European children of 1 to 3.5 y of age (y1-3.5) (Fig. 1*C*). Particularly, the proportion of Vγ9Vδ2$^+$ T cells among all γδ T cells significantly increased from a median of 49% in w1-2 of life to 86% at the second time point of blood collection only a few weeks later (Fig. 1 *D* and *E*). Notably, this increase was observed in every single donor, only differing in magnitude, and was not related to the mother's health status and/or severe pregnancy/birth complications (*SI Appendix*, Fig. S1*D*). Increased Vγ9Vδ2$^+$ T cell frequencies correlated with increased absolute cell numbers at w3-5 (Fig. 1*F*). Most Vγ9Vδ2$^+$ T cells displayed a naïve phenotype reflected by surface expression of CD27 at w1-2, whereas a tendency toward a more activated/memory CD27^{neg} phenotype was evident after 3 to 5 wk (Fig. 1*G*). In contrast, frequencies of Vδ1$^+$ T cells remained stably low and rather decreased in newborns in the first weeks of life (*SI Appendix*, Fig. S1*A*), albeit absolute Vδ1$^+$ cell numbers slightly increased (*SI Appendix*, Fig. S1*B*) and their phenotype remained naïve (CD27^{pos}) (*SI Appendix*, Fig. S1*C*). Interestingly, three newborns that were delivered from mothers with preeclampsia were characterized by lower Vγ9Vδ2$^+$ T cell frequencies and higher Vδ1$^+$ T cell frequencies compared to babies from mothers without preeclampsia, but only in w1-2 (*SI Appendix*, Fig. S1*D*). Taken together, FACS analysis of neonatal peripheral blood lymphocytes demonstrated an immediate burst of Vγ9Vδ2$^+$ T cells directly after birth.

Vγ9Vδ2$^+$ T Cells Undergo Polyclonal Proliferation in Newborns. Recent NGS studies revealed that fetal and cord blood γδ TCR repertoires are extremely polyclonal and comprise Vγ9Vδ2$^+$ T cell clones that have simple rearrangements with no or few N insertions (nucleotides) and utilize *TRDJ1*, *TRDJ2*, and in particular *TRDJ3* joining elements (31, 52). In contrast, adult γδ TCR repertoires use varying numbers of N insertions and mainly *TRDJ1* joining elements (31). To understand how many, if not all, of the neonatal Vγ9Vδ2$^+$ T cells were participating in the observed immediate proliferation after birth, we next explored the γδ TCR repertoires of preterm babies (w1-2 and w3-5) via NGS analysis of FACS-sorted γδ T cells. For this, CDR3 regions of either the γ-chains (*TRG*) or δ-chains (*TRD*) were analyzed via an RNA-based NGS approach (37). Overall, *TRG* and *TRD* repertoire diversity in preterm neonates was polyclonal and did not show obvious differences between samples from w1-2 or w3-5 neonates as illustrated by representative treemaps of one donor (Fig. 2*A*). Next, a systematic comparison of TCR repertoire diversity among 1- to 2-wk- and 3- to 5-wk-old preterm neonates was performed by calculating Shannon indices, which take the repertoire size and the clonal distribution into consideration. However, no age-related differences between the diversity of *TRG* and *TRD* repertoires based on Shannon indices were detectable (Fig. 2*B*). In sum, these studies demonstrate that γδ TCR repertoires remain polyclonal in 3- to 5-wk-old preterm neonates. In line with the rapid expansion of neonatal Vγ9Vδ2$^+$

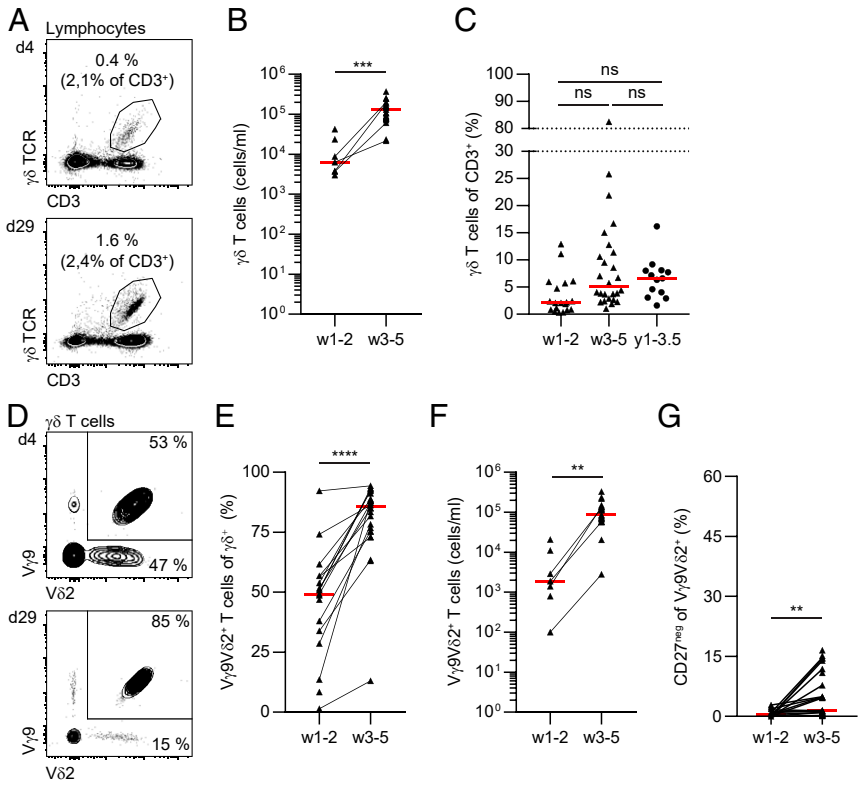

Fig. 1. Flow cytometric analysis reveals immediate burst of Vγ9Vδ2$^+$ T cells within the first 5 wk of life. Peripheral blood γδ T cells of individual preterm newborns were analyzed at weeks 1 to 2 (w1-2) or weeks 3 to 5 (w3-5). (*A*) Representative contour plots of one preterm baby at two time points (d4 and d29). Cells were gated on live (DAPI^{neg}) lymphocytes and frequencies of γδ T cells are indicated. (*B*) Cell numbers of γδ T cells per milliliter of blood from newborns at w1-2 and w3-5 were calculated from lymphocyte counts. (*C*) Frequencies of γδ T cells among CD3$^+$ T cells in PBMCs of all newborns at two time points (w1-2 and w3-5) and in PBMCs of children from 1 to 3.5 y of age (y1-3.5). Median values are represented by lines and individual frequencies by triangles/dots. One-way ANOVA with multiple comparisons by Tukey was performed and no significant difference ($P < 0.05$) was found (ns). (*D*) Representative staining of γδ T cells with anti-Vγ9 and -Vδ2 mAb is shown for one preterm baby (as in *A*) at two time points. (*E*) Vγ9Vδ2$^+$ T cell frequencies of γδ T cells in all preterm neonates at w1-2 and w3-5 are plotted. (*F*) Absolute Vγ9Vδ2$^+$ T cell numbers per milliliter of blood were quantified from blood lymphocytes of preterm neonates at w1-2 and w3-5, if data for lymphocyte counts were available for the participants. (*G*) Frequencies of CD27^{neg} cells among Vγ9Vδ2$^+$ T cells. (*B*, *E*, and *G*) Matched samples of the same donor are connected by black lines, and red lines show median values. (*B*, *E*, and *G*) Statistical analysis was performed by unpaired *t* test (**$P < 0.01$, ***$P < 0.001$, ****$P < 0.0001$).

T cells in our FACS data, the proportion of Vγ9$^+$ and Vδ2$^+$ sequences, represented by *TRGV9* and *TRDV2* usage, significantly increased in γδ TCR repertoires of 3- to 5-wk-old neonates as compared to 1- to 2-wk-old neonates (Fig. 2 *C* and *D*). Next, we showed that the relative frequencies of *TRDJ1*, *TRDJ2*, and *TRDJ3* joining elements among all Vδ2$^+$ sequences (filtered from the total *TRD* sequence pool) remained stable between 1- to 2-wk and 3- to 5-wk neonates (Fig. 2*E*). Moreover, Vδ2$^+$ *TRD* clones similarly used few N insertions (median of 3.8 and 4 nucleotides [nt]) at both time points (Fig. 2*F*). Together, this further supports the idea that a large fraction of all neonatal clones participates in the quick Vγ9Vδ2$^+$ T cell expansion after birth.

Nevertheless, we found evidence for a specific selection of pAg-reactive Vγ9Vδ2$^+$ T cells in the first weeks of life. First, there was a significant increase of hydrophobic amino acids (L, I, and V) at position 97 of all Vδ2$^+$ *TRD* clones, a position that has been implicated in pAg sensing (32, 34, 51), (Fig. 2*G*). Second, analysis of all Vγ9$^+$ *TRG* clones, filtered from all *TRG* sequences, revealed a significant increase of *TRGJP* usage from a median of 72% in w1-2 neonates to 92% in w3-5 infants (Fig. 2*H*). Third, clones using the canonical pAg-reactive Vγ9JP$^+$ CDR3 amino acid sequence "ALWEVQELGKKIKVF" were increased at the second time point of longitudinal sample collection (Fig. 2*I*). Recently, Papadopoulou et al. (52) described in detail how this germline-encoded Vγ9JP$^+$ clone can rearrange using the short-homology repeat GCA in the absence of N insertions in the fetal thymus, thereby generating a specific nucleotide sequence (nucleotype) containing the GT**G** (V) **CA**A (Q) motif. Here, we explored the presence of this fetal-derived Vγ9JP$^+$ nucleotype and could show an increase of the fetal-derived nucleotide sequences in w3-5 neonates, indicating a role in the observed expansion of Vγ9Vδ2$^+$ T cells (Fig. 2*J*).

Summarized, the NGS studies importantly extend our FACS data by demonstrating that the rapid expansion of Vγ9Vδ2$^+$ T cells within the first weeks of life is polyclonal and comes along with a selection of pAg-reactive clones defined by characteristic features of Vγ9JP and Vδ2 chains.

Public, Innate Vδ2$^+$ *TRD* Clones Expand in Neonates and Persist in Children from Europe and Africa. Next, we investigated γδ TCR repertoires in older children and the influence of different geographical locations on repertoire composition. For this, we compared γδ TCR repertoires of European (E) preterm neonates (w1-2 and w3-5) to those of 1- to 3.5-y-old European children (y1-3.5) and of 9-mo-old infants from The Gambia, West Africa (m9 [A]) (*SI Appendix*, Table S1 and S2). Overall, there was evidence for a polyclonal distribution and a relatively high prevalence of Vγ9JP$^+$ sequences in the majority of 1- to 3.5-y-old European children (*SI Appendix*, Fig. S2). However, 3- to 5-wk-old preterm infants had a relatively homogenous distribution of Vδ2$^+$ clones within total *TRD* repertoires, while more

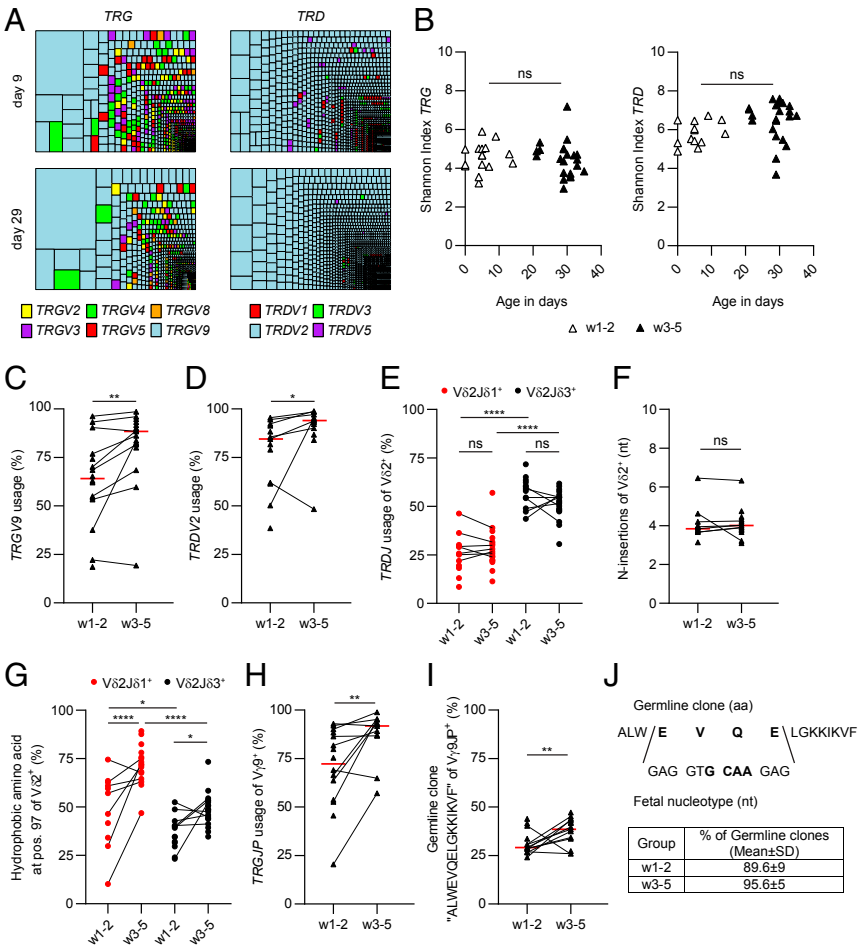

Group	% of Germline clones (Mean±SD)
w1-2	89.6±9
w3-5	95.6±5

Fig. 2. TCR repertoires reflect a rapid polyclonal Vγ9Vδ2$^+$ T cell expansion. *TRD* and *TRG* repertoires of sorted γδ T cells from preterm newborns w1-2 and w3-5 after birth were analyzed by NGS. (*A*) Treemaps show *TRG* and *TRD* clone distribution of one child at day 9 and day 29 after birth, whereas each clone is represented by a box sized according to frequency. Clones are color coded by V-gene usage. (*B*) Shannon indices of *TRG* (*Left*) and *TRD* (*Right*) repertoires dependent on age of preterm newborns at weeks 1 to 2 or weeks 3 to 5. Shannon indices of *TRG* were independent of sorted γδ T cell numbers, whereas those of *TRD* were slightly lower when fewer γδ T cells were sorted (*SI Appendix*, Fig. S2 *A* and *B*). *TRGV9* (*C*) and *TRDV2* (*D*) usage of γδ T cells was calculated from *TRG* and *TRD* repertoires. (*E*) *TRDJ1* (red dots, *Left* side) and *TRDJ3* (black dots, *Right* side) usage of Vδ2$^+$ clones of the *TRD* repertoire at w1-2 and w3-5 after birth. (*F*) N insertions (nucleotides) at the junction of Vδ2 chains at both time points. (*G*) Presence of a hydrophobic amino acid (L, I, or V) at position δ97 as percentage of all Vδ2Jδ1$^+$ (red dots, *Left* side) or Vδ2Jδ3$^+$ (black dots, *Right* side) clones. (*E* and *G*) Matched samples of the same donor are connected by black lines. One-way ANOVA with multiple comparisons by Tukey was performed and significant differences within groups and within time points (e.g., w1-2 of Vδ2Jδ1$^+$ vs. Vδ2Jδ3$^+$) are shown ($^{ns}P > 0.05$, $^*P < 0.05$, $^{****}P < 0.0001$, nonsignificant differences are defined as ns). (*H*) *TRGJP* usage of Vγ9$^+$ clones of the *TRG* repertoire within the respective group. (*I*) Frequencies of germline-encoded clone (CDR3: "ALWEVQELGKKIKVF") of Vγ9JP$^+$ sequences are plotted. (*J*) Mean frequencies ± SD of the fetal nucleotype "GCCTTGTGGGAGGTGCAAGAGTTG-GGCAAAAAAATCAAGGTATTT" encoding the germline clone are shown. (*C*, *D*, *F*, *H*, and *J*) Matched samples of the same donor are connected by black lines, and median values are shown by red lines. Statistical analysis was performed by unpaired *t* test ($^{ns}P > 0.05$, $^*P < 0.05$, $^{**}P < 0.01$, nonsignificant differences are defined as ns).

variable Vδ2$^+$ sequence frequencies were observed in older European and African children (Fig. 3*A*).

Additionally, we filtered *TRD* repertoires for Vδ2$^+$ sequences, observing that *TRDJ* usage was only skewed toward *TRDJ1* with increasing age (Fig. 3*B* and *SI Appendix*, Fig. S3 *A*–*C*). Of note, when analyzing non-Vδ2$^+$ clones, we observed a similar but faster increase in *TRDJ1* usage after birth (*SI Appendix*, Fig. S3*D*). In sum, this suggests that there might already be a shift to an adult-like Vδ2$^+$ *TRD* repertoire in older children that differs from cord blood (31) and from neonates as implied by *TRDJ* usage.

Germline-encoded Vγ9JP$^+$ sequences are present as public *TRG* clones in every single individual, while *TRD* repertoires were described to be highly individual among adults (31, 36, 37). Knowledge about the abundance of shared *TRD* clones in neonates and children remains scarce. We therefore investigated the prevalence of shared *TRD* clones in the preterm neonates and young children from Africa and Europe. First, we estimated *TRD* repertoire similarities between individual study participants using the Morisita–Horn similarity index, where a value of 1 indicates that the two samples are identical and a value of 0 indicates that there is no overlap at all. Morisita–Horn similarity indices between individual samples of the respective study populations increased from w1-2 to w3-5 neonates and declined in 9-mo-old African children as well as in 1- to 3.5-y-old European children (Fig. 3*C*). In brief, this implies an increase of shared clones in the first weeks of life and a lower prevalence in children. A detailed overlap calculation of *TRD* clones (being either Vδ2$^+$ or non-Vδ2$^+$) between samples showed that shared clones are typically Vδ2$^+$ within all child study populations (Fig. 3*D*). Markedly, median values of shared Vδ2$^+$ *TRD* clones at different ages increase in the first 3 wk of life and subsequently decrease in older

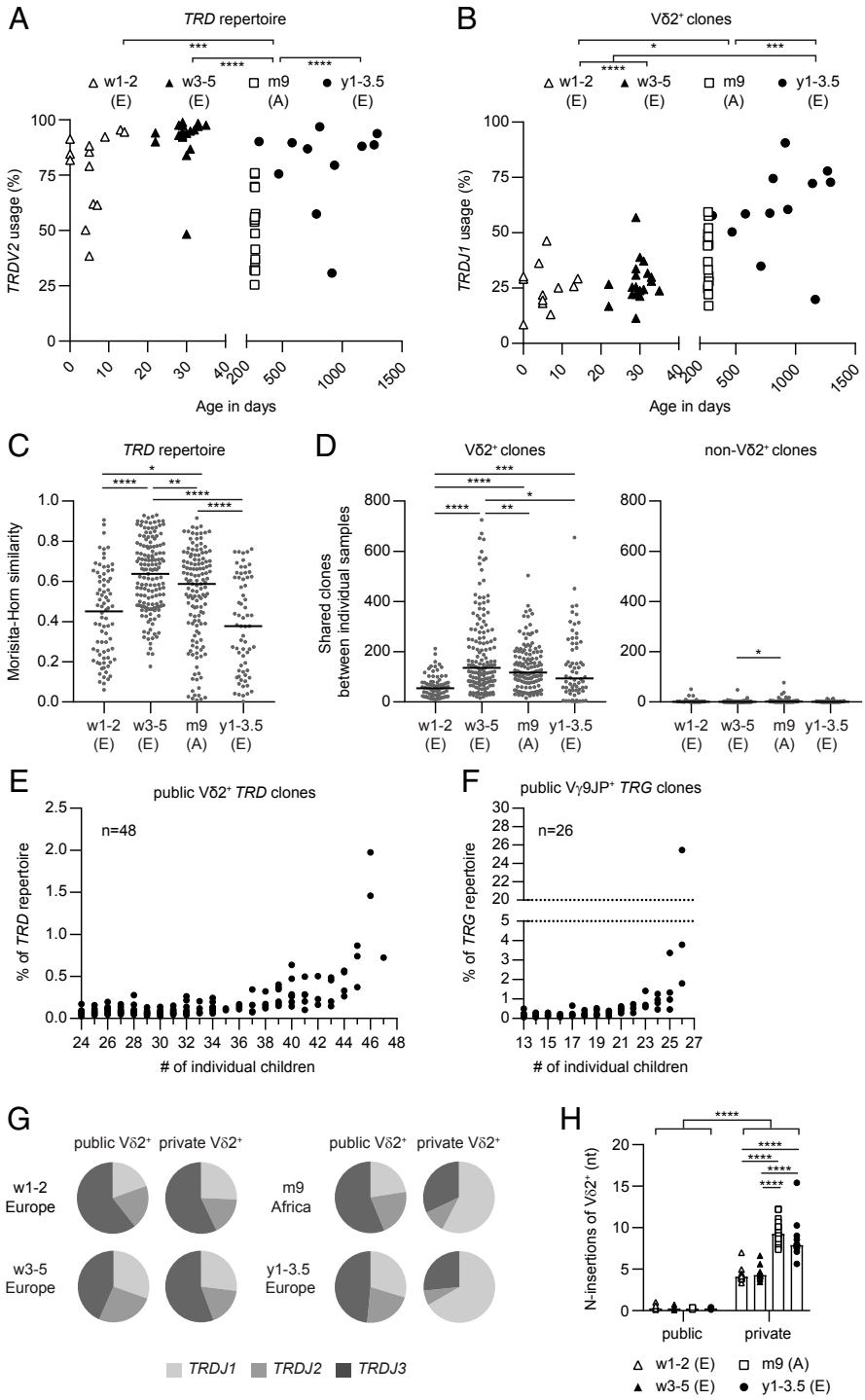

Fig. 3. Fetal-derived, public Vδ2Jδ2/3+ *TRD* clones expand in neonates and persist until childhood. *TRD* repertoires of γδ T cells from 13 European preterm newborns at weeks 1 to 2 after birth (w1-2; E), 18 European preterm newborns at weeks 3 to 5 after birth (w3-5; E), 13 European children being 1 to 3.5 y old (y1-3.5; E) and 17 African children, 9 mo old (m9; A) were analyzed via NGS. (*A*) *TRDV2* usage of pan-γδ *TRD* sequences dependent on age (days) is shown. (*B*) *TRD* repertoires were filtered for Vδ2+ sequences. *TRDJ1* usage of Vδ2+ clones (*TRDV2*) in dependence of age is shown. (*C*) Morisita–Horn similarity indices were calculated between total *TRD* repertoires of individual samples of the respective study populations, while the value 1.0 indicates maximum similarity and 0.0 indicating no similarity at all. Median values are shown in black. (*D*) After filtering all *TRD* sequences for Vδ2+ (*Left*) or non-Vδ2+ sequences (*Right*), the number of shared *TRD* clones within the respective groups was calculated. Medians are depicted by a black line. (*E* and *F*) The number of samples in which each Vδ2+ (*E*) or Vγ9JP+ (*F*) clone was detected is plotted on the *x* axis. Each dot indicates the mean frequency of one clone in all repertoires where it was detected; only clones in more than 50% of datasets (*TRD* >24 datasets/*TRG* >13 datasets) were considered. *TRG* repertoire data were available for 19 preterm neonates (w3-5) and 8 European children (y1-3.5). (*G*) Pie charts indicate proportion of *TRDJ1*, *TRDJ2*, and *TRDJ3* usage among the respective study populations. *TRD* clones were considered public by appearing in at least 50% of samples or private when detected in only one repertoire within the respective study population. (*H*) N insertions (nucleotides) at the junction of Vδ2 chains of public and private clones within the study populations. (*A–D*, *H*) Statistical analysis was performed by one-way ANOVA with Tukey post hoc test (*$P < 0.05$, **$P < 0.01$, ***$P < 0.001$, ****$P < 0.0001$) and nonsignificant differences ($P > 0.05$) are not shown.

children. Importantly, we identified a considerable fraction of Vδ2$^+$ *TRD* clones and Vγ9JP$^+$ *TRG* clones present in at least 50% of all individuals from Europe and Africa (w3-5, m9, and y1-3.5) when cross-comparing all individual samples independent of age (Fig. 3 *E* and *F*). Hence, these specific Vδ2$^+$ *TRD* and Vγ9JP$^+$ *TRG* sequences were defined to be public sequences and further analyzed. The mean frequency of each public Vδ2$^+$ or Vγ9JP$^+$ clone was plotted against the number of samples in which it occurred, revealing that the most shared *TRD* and *TRG* clones were generally more abundant in the respective *TRD* and *TRG* repertoires (Fig. 3 *E* and *F*). Most importantly, these clones were present in all neonates and children irrespective of age and geographical location. Another detailed characterization of public Vδ2$^+$ *TRD* clones (detected in at least 50% of samples) and private Vδ2$^+$ *TRD* clones (present only in one sample) demonstrated that public and private Vδ2$^+$ *TRD* clones in w1-2 and w3-5 neonates used *TRDJ1*, *TRDJ2*, and *TRDJ3* gene elements (Fig. 3*G*). However, later on in childhood (m9 Africa and

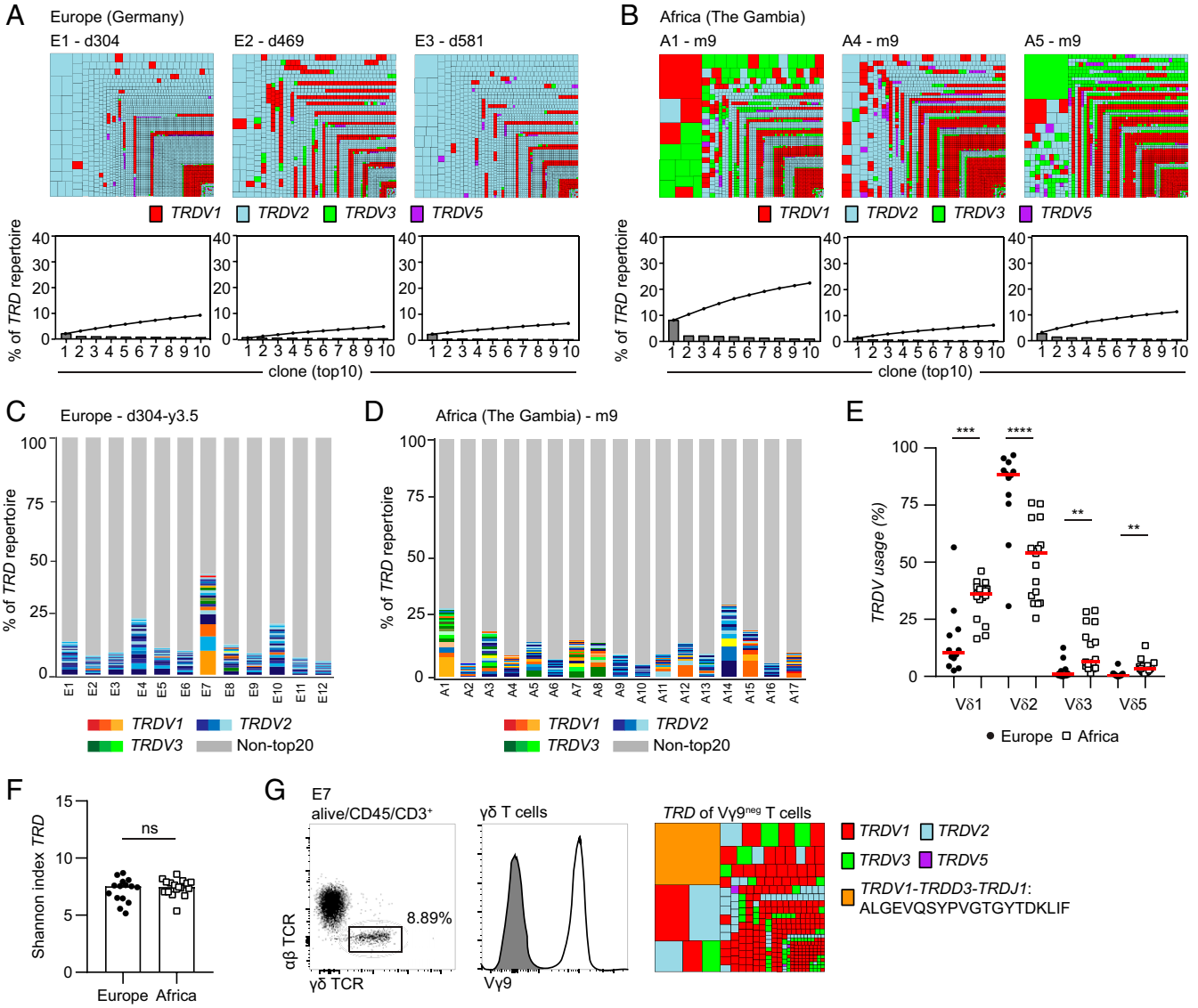

Fig. 4. Non-Vγ9Vδ2$^+$ *TRD* repertoires are differentially shaped in children from Europe and Africa. *TRD* repertoires of total peripheral blood γδ T cells from healthy 1- to 3.5-y-old children living in Europe (E) or 9-mo-old children from The Gambia/West Africa (A samples) were analyzed. (*A* and *B*) Treemaps show *TRD* clone distributions within three representative European children at the age of approximately 1 y (E1-3) and three 9-mo-old African (A) children. Each box represents the abundance of a single clone by its size. V-genes are color coded. In addition, clone frequencies (bars) as well as accumulated frequencies (summed frequencies of bars, illustrated as connected points) of the top10 clones are plotted for each sample in percent of the whole repertoire. (*C* and *D*) Stacked area graphs display the abundance of the most expanded 20 *TRD* clones (top20) within each African (A) and European (E) child. Single clones are represented by boxes sized according to frequency and color coded by V-gene usage (*TRDV1*: red shades; *TRDV2*: blue shades; and *TRDV3*: green shades) and nontop20 clones are highlighted in light gray. (*E*) V-gene usage was calculated for each individual African and European child. (*F*) Dot plot indicates Shannon diversity of the individual *TRD* repertoires. (*E* and *F*) Each dot represents one sample and horizontal lines/bars show median values. (*G*) FACS data representation of γδ T cell frequencies (DAPI^{neg}, CD45$^+$, CD3$^+$) as well as proportions of Vγ9$^+$ and Vγ9^{neg} γδ T cells via dot plots and histogram isolated from PBMCs of a child sampled at day 915 after birth (ID: E7). *TRD* repertoires of Vγ9$^+$ γδ T cells are shown as a treemap (as in *A* and *B*). The most expanded clone (CDR3: "ALGEVQSYPVGTGYTDKLIF") is highlighted in orange. (*E* and *F*) Statistical analysis was performed by unpaired *t* test ($^{ns}P > 0.05$, $^{**}P < 0.01$, $^{***}P < 0.001$, $^{****}P < 0.0001$, nonsignificant differences are defined as ns) in *F*, each *TRDJ* gene was compared between European and African children. Age of children is given in years (y), months (m) or days (d).

y1-3.5 Europe) private *TRD* clones predominantly used *TRDJ1* elements (Fig. 3*G*). In all study populations, the majority of public Vδ2$^+$ *TRD* clones were characterized by insertion of zero or few N insertions and higher numbers in private Vδ2$^+$ *TRD* clones (Fig. 3*H* and *SI Appendix*, Table S4).

In summary, analyzing γδ TCR repertoires of preterm neonates and children from Europe and Africa, we show that γδ TCR repertoires contain public, innate Vδ2$^+$ *TRD* sequences characterized by *TRDJ1/2/3* usage and few N insertions. These public *TRD* sequences presumably pair with Vγ9JP$^+$ sequences and may represent a recently described fetal subset of Vγ9Vδ2$^+$ T cells (52). Our data indicate that this innate Vγ9Vδ2$^+$ T cell subset is characterized by usage of public *TRD* sequences, immediately expands after birth, is highly conserved in all individuals from Europe and Africa, and might be slowly replaced by a more diverse repertoire of Vδ2Jδ1$^+$ T cell clones during childhood.

Differential Microbial Exposure May Shape *TRD* Repertoires in Children Living in Europe or Africa. CMV-induced adaptive-like expansion of individual γδ T cell clones (Vδ1$^+$) was demonstrated in adults (37, 40). However, little is known about other triggers of clonal γδ T cell expansion. Variable V-gene usage in European and Gambian children suggested that individual *TRD* repertoires are already formed in young children (Fig. 3*A*). Hence, we compared in more detail *TRD* repertoires of 1- to 3.5-y-old children from Europe to 9-mo-old children living in The Gambia, Africa. Of note, at the time samples were collected there was a decline of malaria incidence in The Gambia, Africa (53). Comparison of representative *TRD* repertoires via treemaps and the distribution of the 10 most expanded (top10) clones revealed that *TRD* repertoires are polyclonal in young children from both Europe and Africa (Fig. 4 *A* and *B*). The proportion of the most abundant 20 (top20) clones within each individual child further indicated largely polyclonal TCR repertoires in both populations (Fig. 4 *C* and *D*). Remarkably, some individuals (e.g., A1, A12, and A15) from The Gambia and one European child (E7) showed (moderate) expansion of Vδ1$^+$ or Vδ3$^+$ *TRD* clones (Fig. 4 *C* and *D*). Interestingly, there was also a systematically higher presence of Vδ1$^+$ and Vδ3$^+$ sequences in the 9-mo-old children from The Gambia, Africa (Fig. 4 *A*–*D*) and V-gene quantification of all samples demonstrated an increase of Vδ1$^+$ and Vδ3$^+$ sequences in children from Africa/The Gambia (Fig. 4*E*). Yet, overall few age-related correlations with respect to the top20 clone distribution were observed in both groups. In line with this, Shannon indices showed similar *TRD* repertoire diversities between samples of the two study populations (Fig. 4*F*).

Although the majority of European children had highly polyclonal *TRD* repertoires consisting of mainly Vδ2$^+$ T cell clones, one child (E7, 915 d of age), hospitalized due to 3-d fever at the age of 1 y, could be distinguished by expansion of one distinct Vδ1$^+$ T cell clone (Fig. 4 *C* and *G*). At day 915 after birth, a relatively high γδ T cell frequency among lymphocytes (8%) was

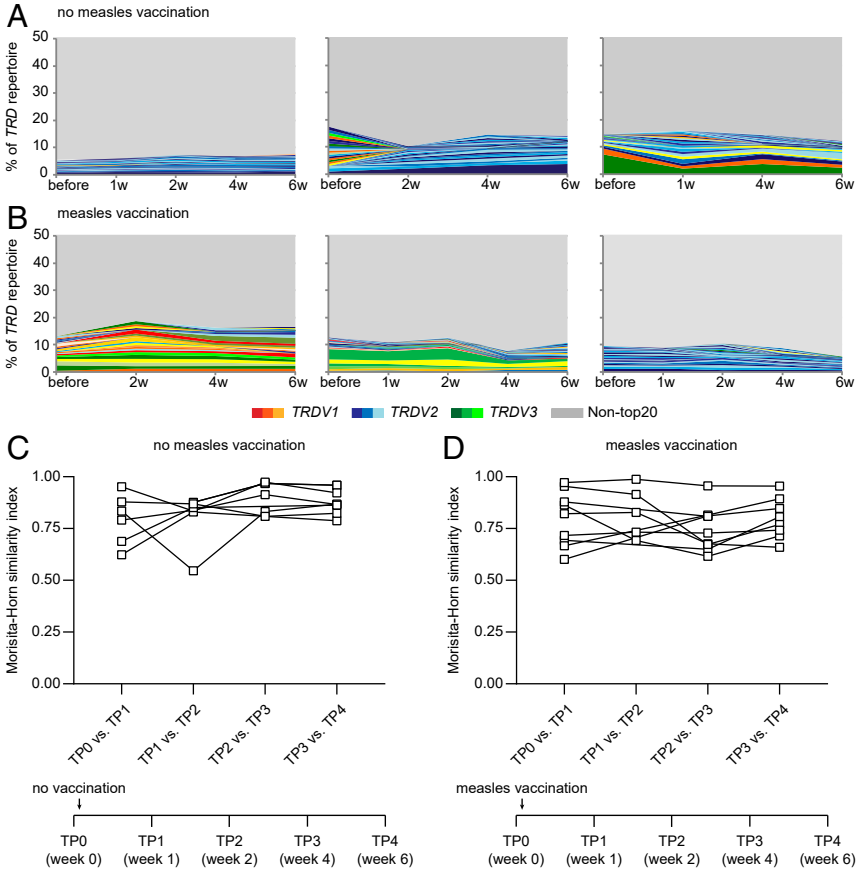

Fig. 5. *TRD* repertoires stay stable after measles vaccination. *TRD* repertoires of healthy 9-mo-old African children from The Gambia were monitored before and after measles vaccination. (*A* and *B*) Stacked area graphs highlight the distribution and overlap of top20 clones before and 1, 2, 4, and 6 wk after measles vaccination within three representative children and (*B*) in three children not receiving a measles vaccination (*A*). Single clones are represented by boxes sized according to frequency and color coded by V-gene usage (*TRDV1*: red shades; *TRDV2*: blue shades; and *TRDV3*: green shades). Nontop20 clones are shown in light gray. (*C* and *D*) Morisita–Horn similarity indices were calculated between indicated time points of each donor while an index of 1.0 represents highest similarity and 0.0 no similarity at all.

observed in this child and a potential footprint of this febrile event was visible in the clonal expansion of Vδ1$^+$ T cell clones within sorted Vγ9^{neg} T cells (Fig. 4*G*).

To investigate whether minor immune challenges like vaccinations could change γδ TCR repertoires, we monitored how measles vaccination, i.e., a controlled attenuated infection challenge, may influence γδ T cells. For this, *TRD* repertoires of peripheral blood γδ T cells from 9-mo-old children from Africa (The Gambia) were analyzed before and up to 6 wk after receiving a live-attenuated measles vaccination. These *TRD* repertoires stayed relatively stable, as represented by the distribution and overlap of the most expanded top20 clones (consisting of Vδ2$^+$ and non-Vδ2$^+$ sequences) before and at different time points after vaccination within representative vaccinated and nonvaccinated children as a control group (Fig. 5 *A* and *B*). Thus, γδ TCR repertoires display a relatively high stability in a defined period of time, which is further reflected in the overall Morisita–Horn similarity indices of *TRD* repertoires calculated between samples of the different time points within the respective donors (Fig. 5 *C* and *D*). Altogether, *TRD* repertoires show similarities (clonality) and differences (enrichment of Vδ1$^+$/Vδ3$^+$ sequences) between children living in Europe and Africa. Moreover, Vδ1$^+$ T cells may expand in response to infectious diseases while live measles vaccination did not significantly affect γδ TCR repertoires.

Children with Febrile Diseases Have Higher γδ T Cell Frequencies. To gain further insights into potential environmental factors causing the (oligo)clonal expansion of non-Vγ9Vδ2$^+$ *TRD* clones, we next analyzed γδ T cells in the peripheral blood of children aged between 0.5 and 14 y that were hospitalized due to fever (above 38.5 °C body temperature) in Danfa, Ghana (*SI Appendix*, Table S3). Notably, acute *P. falciparum* infection was excluded in the febrile children, but individual causes of fever were not recorded. γδ T cells of febrile children were compared to healthy 2- to

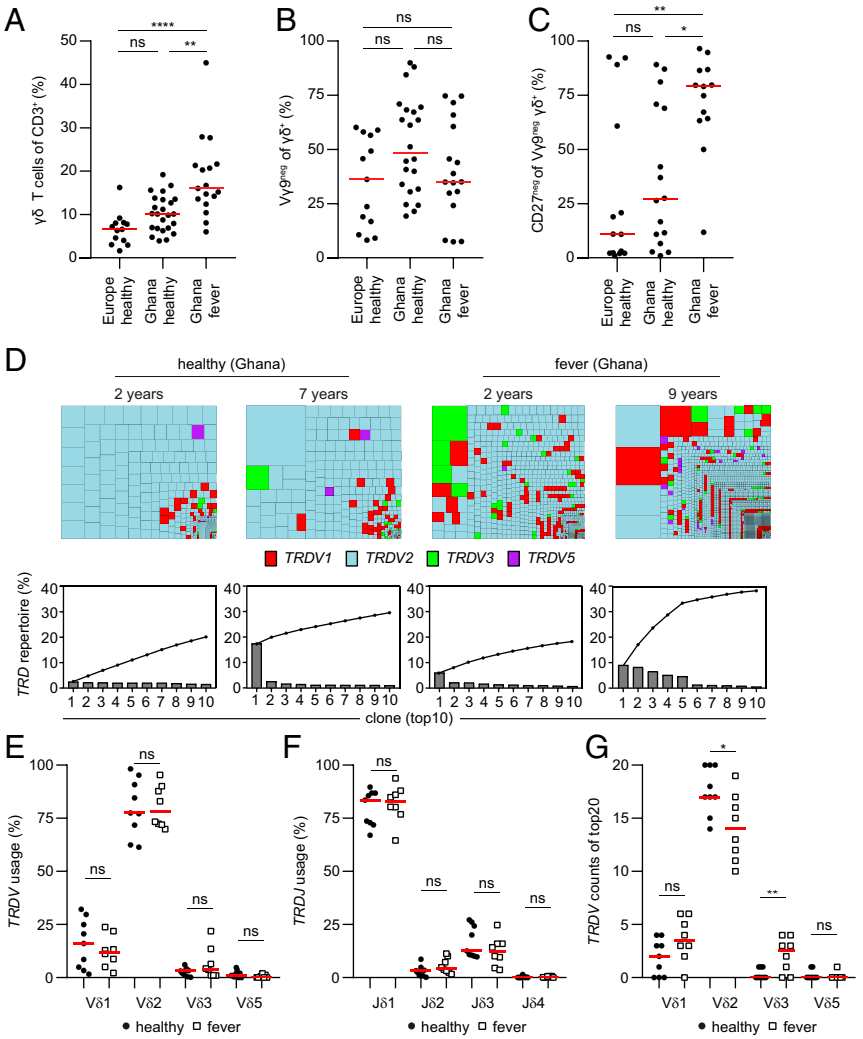

Fig. 6. γδ T cells are more abundant in young children with acute febrile diseases. (*A*) Quantification of γδ T cell frequencies of CD3$^+$ lymphocytes within healthy European children, healthy children from Ghana, and febrile children from Ghana. Data of European children are the same as in Fig. 1*C*. (*B* and *C*) Vγ9^{neg} frequencies of γδ T cells (*B*) and CD27^{neg} of Vγ9^{neg} γδ T cells (*C*) are plotted for the respective child study population. (*A–C*) Each dot indicates one sample and horizontal lines display median values. (*D–G*) *TRD* repertoires of healthy ($n = 9$) and febrile ($n = 8$) Ghanaian children were analyzed via NGS. (*D*) Treemaps and the distribution of top10 clone frequencies (gray bars) and accumulated frequencies of clones (connected points) of two age-matched representative samples are shown. In treemaps each square indicates one clone sized according to frequency. V-gene usage is color coded. (*E–G*) *TRDV* gene usage (*E*) and *TRDJ* gene usage (*F*) as well as counts of *TRDV* genes in top20 clones (*G*) were calculated and median values are indicated by red lines. Statistical analysis was performed by one-way ANOVA with Tukey post hoc test (*A–C*) or by comparing each *TRDV* or *TRDJ* gene between groups with an unpaired *t* test (*E–G*). Levels of significance are indicated ($^{ns}P > 0.05$, $^{*}P < 0.05$, $^{**}P < 0.01$, $^{****}P < 0.0001$, nonsignificant differences are defined as ns).

11-y-old children living in Asutsuare or Owusem which are adjoining communities in the Shai Osudoku District of Ghana, West Africa (malaria prevalence during the study period was 8.9%) (54) and healthy European 1- to 3.5-y-old children. Flow cytometric analysis demonstrated higher γδ T cell frequencies in healthy children from Ghana as compared to European children, and Ghanaian children hospitalized due to acute fever had even higher γδ T cell frequencies (Fig. 6*A*). The abundance of $V\gamma9^{neg}$ T cells varied among children, but overall there was no significant difference between the groups (Fig. 6*B*). The majority of $V\gamma9^{neg}$ γδ T cells in febrile Ghanaian children appeared to have a $CD27^{neg}$ phenotype (median of 79%) as compared to healthy Ghanaian (median of 27%) and healthy European children (median of 11%) (Fig. 6*C*). When analyzing the *TRD* repertoire, no major differences in the clonal distribution between age-matched healthy and febrile Ghanaian children were observed, as illustrated by treemaps as well as accumulated frequencies of top10 clones (Fig. 6*D*). There was also no difference in the distribution of V genes and J genes among healthy and febrile children (Fig. 6 *E* and *F*); however, most of the febrile children showed a higher prevalence of $V\delta1^+/V\delta3^+$ clones in the top20 clones (Fig. 6*G*).

Discussion

Directly after birth, (preterm) neonates start to establish their individual dermal and gastrointestinal microbiota, thought to be the main source of γδ T cell-stimulating pAgs. Thus, it was postulated that $V\gamma9V\delta2^+$ T cells undergo a postnatal expansion in children to become the main γδ T cell subset in the peripheral blood of adults (27, 28). In these published studies, children were mainly observed between 1 and 10 y of age and samples of newborns were rare. Here, we analyzed matched samples of preterm babies shortly after birth and approximately 4 wk later. Strikingly, already by 4 wk of age $V\gamma9V\delta2^+$ T cells were increased in numbers to reach up to 90% of the γδ T cell compartment, revealing a rapid proliferation immediately after birth. This increase was observed in every individual and independent of the mother's health status. Interestingly, we observed low $V\gamma9V\delta2^+$ T cell frequencies and increased $V\delta1^+$ frequencies in preterm newborns directly after birth from mothers diagnosed with preeclampsia. Due to limited sample numbers of such children in our study, future research needs to address whether this constellation of γδ T cell subsets is a consequence or even a pathogenic factor of preeclampsia.

Supported by the fact that γδ T cells are intrinsically primed for effector functions during fetal thymic development (7), a high IFN-γ production capacity of γδ T cells was reported in term and preterm neonates at birth (9). Environmental influences selectively enhanced the TNFα production of γδ T cells, but not αβ T cells, in 1-mo-old preterm neonates (9). Moreover, an effector/memory formation of $V\delta2^+$, but not $V\delta1^+$ γδ T cells from neonates (cord blood) to 14-mo-old children was shown (28). In our study, the majority of $V\gamma9V\delta2^+$ T cells displayed a naïve phenotype ($CD27^+$) at preterm birth, and CD27 expression slightly declined by 4 wk. Taken together, the observed expansion of $V\gamma9V\delta2^+$ T cells highlights selective and dynamic changes in the neonates' γδ T cell compartment immediately after birth, suggesting that $V\gamma9V\delta2^+$ T cells are an important functional subset of the immune system in preterm and term babies.

NGS analysis of γδ TCR repertoires revealed that the postnatal burst of $V\gamma9V\delta2^+$ T cells is due to polyclonal proliferation. Notably, the recently described fetal-derived nucleotype specific for germline-encoded $V\gamma9JP^+$ *TRG* variants (52) took part in this early pAg-mediated $V\gamma9V\delta2^+$ T cell expansion in preterm neonates but was less abundant in young children. Neonatal *TRD* clones expanded irrespective of *TRDJ* usage in weeks 1 to 2 to weeks 3 to 5 newborns. However, an enrichment of certain hydrophobic amino acid sequences at position δ97, described to be important for pAg sensing (32, 34, 51), was noted 3 to 5 wk after birth. This supports the idea that at least some positive selection of particular pAg-specific *TRD* clones from the total γδ T cell pool occurs immediately after birth, independent of *TRDJ* usage. Similar to in vitro-stimulated cord blood $V\gamma9V\delta2^+$ TCR repertoires (55), there was no selective outgrowth of individual $V\delta2^+$ *TRD* clones in 1-mo-old neonates. Yet, this does not explain the increase of *TRDJ1* elements observed in older children.

Importantly, we identified a large number of $V\delta2^+$ *TRD* clones that are shared among basically all neonates, infants, and young children from Europe and Africa. Therefore, these clones can be described as public $V\delta2^+$ *TRD* clones. The *TRD* sequences of such public clones have TCR characteristics similar to fetal-derived $V\delta2^+$ T cells (52), e.g., few N insertions and a high prevalence of *TRDJ1/2/3* elements. Those characteristics support the idea that, similar to αβ T cells, certain invariant $V\gamma9V\delta2^+$ T cell clones might be generated via convergent recombination during thymic development (56) and that this is independent from the genetic background. In sum, the features of public $V\delta2^+$ *TRD* clones are consistent with the definition "innate-like." Yet, it is unclear if such innate-like, public $V\gamma9V\delta2^+$ T cells already originate in the fetal liver (4). The presence of public $V\delta2^+$ T cell clones in independent study populations of European and African children highlights that fetal-derived, public $V\gamma9V\delta2^+$ T cells persist until early childhood. However, as *TRD* repertoires of children already showed features of adult *TRD* repertoires, e.g., higher *TRDJ1* usage and lower occurrence of public clones, our data suggest that fetal-derived $V\gamma9V\delta2^+$ T cells might slowly be replaced by adult-like $V\gamma9V\delta2^+$ T cells (private $V\delta2J\delta1^+$ clones) during the first years of childhood. Future longitudinal data (≥5 y) of newborn and infants could address the hypothesis that adult-like $V\gamma9V\delta2^+$ T cells either originate from the postnatal thymus (31, 52) and/or are positively selected via recurrent exposure to microbial-derived pAgs during life. With respect to murine γδ T cells, it is evident that a defined microbiota may impact on the postnatal proliferation, peripheral maintenance, and function of some, but not all, innate-like γδ T cells (57–62). Altogether, our data indicate that the immunological challenge imposed by birth, which depicts the passage from a relatively sterile to a nonsterile environment, induces an immediate polyclonal expansion of innate-like human $V\gamma9V\delta2^+$ T cells.

By contrast, NGS studies ascribed an adaptive-like mode of action to the human non-$V\gamma9V\delta2^+$ T cell subset (mainly $V\delta1^+$ T cells) as clonal proliferation and long-term memory formation in response to CMV reactivation in transplant recipients is evident (37, 63). In this context, highly focused $V\delta1^+$ TCR repertoires have been described in CMV^+, but also CMV^{neg} adult individuals (40), indicating that not just CMV infections influence the non-$V\gamma9V\delta2^+$ TCR repertoire. Indeed, we observed expanded $V\delta1^+$ T cell clones in one European child hospitalized due to 3-d fever, which is frequently caused by HHV6/7 infections in very young children (64). Here, we assumed that African children are exposed to a different and potentially richer exposome (microbes, serious pathogens) than European children. First, NGS analysis outlined overall similar *TRD* repertoire diversity between healthy European and Gambian children. Starting with the observation that there is a higher prevalence of $V\delta1^+/V\delta3^+$ T cell clones (oligoclonal distribution) in healthy 9-mo-old African children, flow cytometric analysis further confirmed previous findings that healthy African children have higher γδ T cell frequencies compared to European children (65). A measles vaccination that represents a subclinical infection by an attenuated pathogen in early life did not obviously influence either the $V\gamma9V\delta2^+$ or the non-$V\gamma9V\delta2^+$ TCR repertoire, thereby confirming a high TCR repertoire stability in healthy infants. Hence, we may propose that only strong immunological challenges such as wild-type natural infections

might profoundly impact γδ TCR repertoires. Importantly, γδ T cell frequencies were strikingly increased in children hospitalized in Ghana due to fever. As low CD27 expression was observed on $Vγ9^{neg}$ T cells in almost every individual febrile child, these data proposed that γδ T cells expanded as effector T cells. Unfortunately, associated medical records are incomplete with only infection by *P. falciparum* excluded in these patients and *Klebsiella pneumoniae* detected in the urine of three of these children. However, a number of infections with bacteria, viruses, and parasites were described to result in increased γδ T cell numbers ($Vγ9Vδ2^+$ and/or non-$Vγ9Vδ2^+$ T cells) (66). Finally, it could also be the case that fever per se drives an acute γδ T cell proliferation (67), perhaps indirectly via TCR recognition of heat shock proteins. Future prospective studies should address the influence of specific bacterial, parasitic, and viral infections on the γδ TCR repertoire in young children.

In summary, the observed immediate postnatal expansion of $Vγ9Vδ2^+$ T cells even in preterm neonates highlights their importance in the neonatal immune compartment and their prompt response capabilities to pAgs, which are presumably produced by the newborn's microbiota. We identified a considerable fraction of public, fetal-derived $Vδ2^+$ clones, which used *TRDJ1/2/3* elements in neonates. This subset persists until childhood and appears to be slowly replaced by more private $Vδ2Jδ1^+$ clones during postnatal development, finally resulting in highly individual adult *TRD* repertoires (31, 37). In addition, we provide evidence that non-$Vγ9Vδ2^+$ T cells can expand in response to infectious diseases in young children and their TCR repertoire may serve as a valuable marker of the individual's history of microbial exposure.

Methods

Study Populations and Peripheral Blood Mononuclear Cells Isolation. European infants and young children's peripheral blood mononuclear cells (PBMCs) were freshly isolated by Ficoll-Paque density gradient centrifugation from blood samples obtained from 14 healthy term-born infants and children at the ages of 304 to 1,294 d and from 30 preterm infants born at a gestational age of 26 to 32 weeks (PRIMAL cohort) (68), excluding only preterm infants with lethal abnormalities (*SI Appendix*, Table S1). Four mothers of four preterm infants (from which we collected six blood samples) were diagnosed with preeclampsia. One mother of one preterm infant (from which we collected one blood sample) was a renal and liver graft recipient and on immunosuppressive treatment. All remaining mothers of term (n = 14) and preterm (n = 25) infants were healthy and had no overt pregnancy and/or birth complications. In all preterm infants the first blood sample used in this study was collected in w1-2 of life; in 15 of these preterm infants a second blood sample collected in w3-5 of life was used. Isolated PBMCs were directly used for cell sorting. Blood drawings were done in the Department of Pediatrics, Hannover Medical School, and have been approved by the Institutional Review Board of the Hannover Medical School (nos. 6031–2011, 6031–2015, and 8014_BO_S_2018).

The Gambia (Africa) study (*SI Appendix*, Table S2) was approved by the Gambian Government/MRC Joint Ethics Committee, and The London School of Hygiene and Tropical Medicine Ethics Committee (study no. SCC1085). Samples were collected from 9-mo-old infants presenting for routine immunization. For malaria prevention, women took intermittent malaria treatment during pregnancy with sulfadoxine/pyrimethamine and used bed nets. Hence, pregnancy infection rates were presumably relatively low too. Infants were randomized into one of two groups: one group received a single intramuscular dose of measles vaccine (MV) (Edmonston Zagreb, Serum Institute of India Ltd, Pune, India) into the right deltoid (n = 11) and the other group received no vaccine (n = 6). All children were afebrile and healthy on the day of admission. Children were bled on the day of recruitment prior to immunization and then 1 wk, 2 wk, 4 wk, and 6 wk later. On each occasion a 500 μL whole blood sample was collected directly into a PAXgene blood RNA tube and stored at −80 °C for later RNA extraction.

For samples collected in Ghana (Africa) (*SI Appendix*, Table S3), the study was approved by the Institutional Review Board of Noguchi Memorial Institute for Medical Research (NMIMR) of the University of Ghana, Accra, Ghana (NMIMR-IRB CPN 028/07–08 and CPN 109/15–16 amendment 2017). Ghanaian samples were either collected in Asutsuare or Owusem (for healthy children) or Danfa (febrile children were defined by a body temperature above 38.5 °C) and malaria blood slide microscopy negative for any *P. falciparum* parasites which is the gold standard for malaria diagnosis in the hospitals in Ghana). Samples were processed at the Immunology Department of NMIMR. Briefly, PBMCs were isolated from the peripheral blood by density gradient cell separation using Ficoll Paque Plus and enumerated with a hemocytometer, following freezing in RPMI, 10% fetal calf serum (FCS), penicillin/streptomycin, and 10% dimethyl solfoxide (DMSO).

Written informed consent was provided by the parents or guardians of all participants before they were enrolled into the study.

Flow Cytometric Analysis and Sorting. Fresh or thawed PBMCs were washed in phosphate-buffered saline (PBS) with 5% FCS, incubated for 5 min in 5% Fc-receptor block, following antibody incubation for 20 min on ice for flow cytometric analysis and cell sorting. Dead cells were detected via DAPI staining. The following antibodies were used: anti-CD3 FITC (clone REA613; Miltenyi Biotec), anti-CD3 PE-Cy7 (clone SK7; BD Bioscience), anti-γδ TCR PE (clone 11F2, BD Bioscience or Miltenyi Biotec), anti-αβTCR APC-Cy7 (clone BW242/412; Miltenyi Biotec), anti-Vγ9 PE-Cy5 (clone IMMU 360; Beckman Coulter), anti-Vγ9 FITC (clone IMMU 360; Beckman Coulter), anti-Vδ2 APC (clone 123R3; Miltenyi Biotec), anti-Vδ1 VioGreen (clone REA173; Miltenyi Biotec), anti-CD27 PE-Cy7 (clone LG.7F9, eBioscience), and anti-CD27 AF700 (clone O323; BioLegend). Neonatal samples were only sorted for living/$CD3^+$/$αβTCR^{neg}$ γδ T cells, whereas samples of children were either sorted for total γδ T cells or divided into $Vγ9^+$ and $Vγ9^{neg}$ γδ T cells. Cells were sorted on a FACSAria Fusion Cell Sorter (BD Bioscience). Samples of the PRIMAL cohort were sorted for living/$CD3^+$/$γδ\ TCR^+$ cells. Flow cytometric data were analyzed using FlowJo software v10 (Tree Star).

Absolute cell numbers were calculated using lymphocyte counts per microliter and flow cytometry data.

TCR Amplicon Generation and NGS. FACS-sorted γδ T cells, $Vγ9^+$, or $Vγ9^{neg}$ γδ T cells of preterm babies (1 to 2 wk or 3 to 5 wk after birth), European children (1 to 3.5 y), and Ghanaian children (2 to 14 y) were lysed in RLT lysis buffer (Qiagen) after adding isolated mouse thymocytes for spike-in. The RNAeasy Micro Kit (Qiagen) was used for RNA isolation. Either 10 μL RNA of total γδ T cells or 5 μL of $Vγ9^+$ and 5 μL of $Vγ9^{neg}$ γδ T cells were pooled in equal amounts for cDNA synthesis (Superscript III, Invitrogen). For samples of 9-mo-old infants from The Gambia, RNA was isolated from PAXgene blood RNA tube, following reverse transcription (Superscript III, Invitrogen). CDR3 regions of either the γ-chain (*TRG*) or δ-chain (*TRD*) were amplified via gene-specific primer targeting all productive V genes using maximal 35 PCR cycles as previously described (37). Primer sequences for multiplex PCR are as follows: h*TRD*V1: TCAAGAAAGCAGCGAAATCC; h*TRD*V2: ATTGCAAAGAACCTGGCTGT; h*TRD*V3: CGGTTTTCTGTGAAACACATTC; h*TRD*V5/29: ACAAAAGTGCCAAGCACCTC; h*TRD*C1: GACAAAAACGGATGGTTTGG; h*TRG*V (2–5, 8): ACCTACACCAGGAGGGGAAG; h*TRG*V9: TCGAGAGAGACCTGGTGAAGT; and h*TRG*C (1, 2): GGGGAAACATCTGCATCAAG. Moreover, Illumina adaptor sequences (GTCTCGTGGGCTCGGAGATGTGTATAAGAGACAG and TCGTCGGCAGCGTCAGATGTGTATAAGAGACAG) were added as overhangs for all primers.

According to Illumina guidelines, samples were labeled with Nextera XT indices and subjected to paired-end Illumina MiSeq analysis using 500 cycles. A total of 20% PhIX (bacteriophage X) genome was added as sequencing control. Demultiplexed read 1 files were processed for downstream analysis.

Data Analysis. Obtained fastq read files were annotated according to international immunogenetics information system (IMGT) using MiXCR software (69). Annotated read files were processed and analyzed using VDJTools (70) and the TcR package (71). Shannon diversity indices were calculated with the R library Vegan with prior normalization to 17,000 (TRD) or 13,000 (TRG) reads. Treemaps were plotted using the R package Treemap. All bioinformatics analysis was performed using R versions 3.6.0 and bash shell commands.

Statistical Information. Statistical analysis was conducted with the program GraphPad Prism version 8. Statistical analysis was performed by using either unpaired t test or one-way ANOVA with Tukey post hoc test.

Data Availability. FASTQ files of *TRG* and *TRD* sequences are deposited and available under the Bioproject PRJNA592548 (https://www.ncbi.nlm.nih.gov/bioproject/PRJNA592548). Further information about data and reagents used is available by request to the corresponding author.

ACKNOWLEDGMENTS. We thank Matthias Ballmaier of the Hannover Medical School cell sorting facility for support. The study was supported by the German Research Foundation Deutsche Forschungsgemeinschaft

(DFG) under Germany's Excellence Strategy, EXC 2155 "RESIST," Project ID 390874280 to I.P., D.V., and S.R.; the SFB900 Project ID 158989968 to I.P. and S.R.; and the DFG-funded research group FOR2799, Project RA3077/1-1 to S.R. and PR727/11-1 to I.P. This study was supported by the UK Medical Research Council (MRC) (Grant G0701291) awarded to K.L.F., P.D., and P.G.; and as part of an MRC-funded 5-y program grant (2007 to 2011) to the MRC Unit The Gambia (Grant SCC1085) awarded to K.L.F.

1. S. Basha, N. Surendran, M. Pichichero, Immune responses in neonates. *Expert Rev. Clin. Immunol.* **10**, 1171–1184 (2014).
2. I. Debock, V. Flamand, Unbalanced neonatal CD4+ T-cell immunity. *Front. Immunol.* **5**, 393 (2014).
3. T. R. Kollmann, B. Kampmann, S. K. Mazmanian, A. Marchant, O. Levy, Protecting the newborn and young infant from infectious diseases: Lessons from immune ontogeny. *Immunity* **46**, 350–363 (2017).
4. L. D. McVay, S. R. Carding, Extrathymic origin of human gamma delta T cells during fetal development. *J. Immunol.* **157**, 2873–2882 (1996).
5. L. D. McVay, S. S. Jaswal, C. Kennedy, A. Hayday, S. R. Carding, The generation of human gammadelta T cell repertoires during fetal development. *J. Immunol.* **160**, 5851–5860 (1998).
6. P. Tieppo *et al*., The human fetal thymus generates invariant effector γδ T cells. *J. Exp. Med.* **217**, jem.20190580 (2020).
7. T. Dimova *et al*., Effector Vγ9Vδ2 T cells dominate the human fetal γδ T-cell repertoire. *Proc. Natl. Acad. Sci. U.S.A.* **112**, E556–E565 (2015).
8. D. Vermijlen *et al*., Human cytomegalovirus elicits fetal gammadelta T cell responses in utero. *J. Exp. Med.* **207**, 807–821 (2010).
9. D. L. Gibbons *et al*., Neonates harbour highly active gammadelta T cells with selective impairments in preterm infants. *Eur. J. Immunol.* **39**, 1794–1806 (2009).
10. E. Moens *et al*., IL-23R and TCR signaling drives the generation of neonatal Vgamma9Vdelta2 T cells expressing high levels of cytotoxic mediators and producing IFN-gamma and IL-17. *J. Leukoc. Biol.* **89**, 743–752 (2011).
11. C. Cairo *et al*., Cord blood Vγ2Vδ2 T cells provide a molecular marker for the influence of pregnancy-associated malaria on neonatal immunity. *J. Infect. Dis.* **209**, 1653–1662 (2014).
12. A. C. Hayday, γδ T cell update: Adaptate orchestrators of immune surveillance. *J. Immunol.* **203**, 311–320 (2019).
13. D. Vermijlen, I. Prinz, Ontogeny of innate T lymphocytes–Some innate lymphocytes are more innate than others. *Front. Immunol.* **5**, 486 (2014).
14. P. Vantourout, A. Hayday, Six-of-the-best: Unique contributions of γδ T cells to immunology. *Nat. Rev. Immunol.* **13**, 88–100 (2013).
15. Y. H. Chien, Y. Konigshofer, Antigen recognition by gammadelta T cells. *Immunol. Rev.* **215**, 46–58 (2007).
16. A. S. Fichtner, S. Ravens, I. Prinz, Human γδ TCR repertoires in health and disease. *Cells* **9**, 800 (2020).
17. M. M. Karunakaran *et al*., Butyrophilin-2A1 directly binds germline-encoded regions of the Vγ9Vδ2 TCR and is essential for phosphoantigen sensing. *Immunity* **52**, 487–498.e6 (2020).
18. M. Rigau *et al*., Butyrophilin 2A1 is essential for phosphoantigen reactivity by γδ T cells. *Science* **367**, eaay5516 (2020).
19. C. Harly *et al*., Key implication of CD277/butyrophilin-3 (BTN3A) in cellular stress sensing by a major human γδ T-cell subset. *Blood* **120**, 2269–2279 (2012).
20. M. Eberl *et al*., Microbial isoprenoid biosynthesis and human gammadelta T cell activation. *FEBS Lett.* **544**, 4–10 (2003).
21. A. Sandstrom *et al*., The intracellular B30.2 domain of butyrophilin 3A1 binds phosphoantigens to mediate activation of human Vγ9Vδ2 T cells. *Immunity* **40**, 490–500 (2014).
22. S. Vavassori *et al*., Butyrophilin 3A1 binds phosphorylated antigens and stimulates human γδ T cells. *Nat. Immunol.* **14**, 908–916 (2013).
23. K.-J. Puan *et al*., Preferential recognition of a microbial metabolite by human Vgamma2Vdelta2 T cells. *Int. Immunol.* **19**, 657–673 (2007).
24. M. Hintz *et al*., Identification of (E)-4-hydroxy-3-methyl-but-2-enyl pyrophosphate as a major activator for human gammadelta T cells in Escherichia coli. *FEBS Lett.* **509**, 317–322 (2001).
25. C. T. Morita, C. Jin, G. Sarikonda, H. Wang, Nonpeptide antigens, presentation mechanisms, and immunological memory of human Vgamma2Vdelta2 T cells: Discriminating friend from foe through the recognition of prenyl pyrophosphate antigens. *Immunol. Rev.* **215**, 59–76 (2007).
26. R. C. Robertson, A. R. Manges, B. B. Finlay, A. J. Prendergast, The human microbiome and child growth–First 1000 days and beyond. *Trends Microbiol.* **27**, 131–147 (2019).
27. C. M. C. M. Parker *et al*., Evidence for extrathymic changes in the T cell receptor gamma/delta repertoire. *J. Exp. Med.* **171**, 1597–1612 (1990).
28. S. C. De Rosa *et al*., Ontogeny of γ δ T cells in humans. *J. Immunol.* **172**, 1637–1645 (2004).
29. C. R. Willcox, M. S. Davey, B. E. Willcox, Development and selection of the human Vγ9Vδ2$^+$ T-cell repertoire. *Front. Immunol.* **9**, 1501 (2018).
30. M. H. Delfau, A. J. Hance, D. Lecossier, E. Vilmer, B. Grandchamp, Restricted diversity of V gamma 9-JP rearrangements in unstimulated human gamma/delta T lymphocytes. *Eur. J. Immunol.* **22**, 2437–2443 (1992).
31. M. S. Davey *et al*., The human Vδ2$^+$ T-cell compartment comprises distinct innate-like Vγ9$^+$ and adaptive Vγ9$^-$ subsets. *Nat. Commun.* **9**, 1760 (2018).
32. H. Wang, Z. Fang, C. T. Morita, Vgamma2Vdelta2 T Cell Receptor recognition of prenyl pyrophosphates is dependent on all CDRs. *J. Immunol.* **184**, 6209–6222 (2010).
33. F. Miyagawa *et al*., Essential contribution of germline-encoded lysine residues in Jgamma1.2 segment to the recognition of nonpeptide antigens by human gammadelta T cells. *J. Immunol.* **167**, 6773–6779 (2001).
34. S. Yamashita, Y. Tanaka, M. Harazaki, B. Mikami, N. Minato, Recognition mechanism of non-peptide antigens by human gammadelta T cells. *Int. Immunol.* **15**, 1301–1307 (2003).
35. J. F. Bukowski, C. T. Morita, H. Band, M. B. Brenner, Crucial role of TCR gamma chain junctional region in prenyl pyrophosphate antigen recognition by gamma delta T cells. *J. Immunol.* **161**, 286–293 (1998).
36. A. M. Sherwood *et al*., Deep sequencing of the human TCRγ and TCRβ repertoires suggests that TCRβ rearranges after αβ and γδ T cell commitment. *Sci. Transl. Med.* **3**, 90ra61 (2011).
37. S. Ravens *et al*., Human γδ T cells are quickly reconstituted after stem-cell transplantation and show adaptive clonal expansion in response to viral infection. *Nat. Immunol.* **18**, 393–401 (2017).
38. C. T. Morita, C. M. Parker, M. B. Brenner, H. Band, TCR usage and functional capabilities of human gamma delta T cells at birth. *J. Immunol.* **153**, 3979–3988 (1994).
39. J. C. Ribot, S. T. Ribeiro, D. V. Correia, A. E. Sousa, B. Silva-Santos, Human γδ thymocytes are functionally immature and differentiate into cytotoxic type 1 effector T cells upon IL-2/IL-15 signaling. *J. Immunol.* **192**, 2237–2243 (2014).
40. M. S. Davey *et al*., Clonal selection in the human Vδ1 T cell repertoire indicates γδ TCR-dependent adaptive immune surveillance. *Nat. Commun.* **8**, 14760 (2017).
41. B. Di Lorenzo, S. Ravens, B. Silva-Santos, High-throughput analysis of the human thymic Vδ1$^+$ T cell receptor repertoire. *Sci. Data* **6**, 115 (2019).
42. C. R. Willcox *et al*., Cytomegalovirus and tumor stress surveillance by binding of a human γδ T cell antigen receptor to endothelial protein C receptor. *Nat. Immunol.* **13**, 872–879 (2012).
43. R. Marlin *et al*., Sensing of cell stress by human γδ TCR-dependent recognition of annexin A2. *Proc. Natl. Acad. Sci. U.S.A.* **114**, 3163–3168 (2017).
44. J. Le Nours *et al*., A class of γδ T cell receptors recognize the underside of the antigen-presenting molecule MR1. *Science* **366**, 1522–1527 (2019).
45. K. Wistuba-Hamprecht, D. Frasca, B. Blomberg, G. Pawelec, E. Derhovanessian, Age-associated alterations in γδ T-cells are present predominantly in individuals infected with Cytomegalovirus. *Immun. Ageing* **10**, 26 (2013).
46. J. Déchanet *et al*., Implication of gammadelta T cells in the human immune response to cytomegalovirus. *J. Clin. Invest.* **103**, 1437–1449 (1999).
47. F. Halary *et al*., Shared reactivity of Vδ2(neg) γδ T cells against cytomegalovirus-infected cells and tumor intestinal epithelial cells. *J. Exp. Med.* **201**, 1567–1578 (2005).
48. A. Knight *et al*., The role of Vδ2-negative γδ T cells during cytomegalovirus reactivation in recipients of allogeneic stem cell transplantation. *Blood* **116**, 2164–2172 (2010).
49. M. S. Davey, C. R. Willcox, A. T. Baker, S. Hunter, B. E. Willcox, Recasting human Vδ1 lymphocytes in an adaptive role. *Trends Immunol.* **39**, 446–459 (2018).
50. C. Cairo *et al*., Impact of age, gender, and race on circulating γδ T cells. *Hum. Immunol.* **71**, 968–975 (2010).
51. F. Davodeau *et al*., Peripheral selection of antigen receptor junctional features in a major human γ δ subset. *Eur. J. Immunol.* **23**, 804–808 (1993).
52. M. Papadopoulou *et al*., TCR sequencing reveals the distinct development of fetal and adult human Vγ9Vδ2 T cells. *J. Immunol.* **203**, 1468–1479 (2019).
53. S. J. Ceesay *et al*., Continued decline of malaria in the Gambia with implications for elimination. *PLoS One* **5**, e12242 (2010).
54. B. Adu *et al*., Fc γ receptor IIIB (FcγRIIIB) polymorphisms are associated with clinical malaria in Ghanaian children. *PLoS One* **7**, e46197 (2012).
55. A. S. Fichtner *et al*., TCR repertoire analysis reveals phosphoantigen-induced polyclonal proliferation of Vγ9Vδ2 T cells in neonates and adults. *J. Leukoc. Biol.* **107**, 1023–1032 (2020).
56. M. F. Quigley *et al*., Convergent recombination shapes the clonotypic landscape of the naive T-cell repertoire. *Proc. Natl. Acad. Sci. U.S.A.* **107**, 19414–19419 (2010).
57. J. Duan, H. Chung, E. Troy, D. L. Kasper, Microbial colonization drives expansion of IL-1 receptor 1-expressing and IL-17-producing γ/δ T cells. *Cell Host Microbe* **7**, 140–150 (2010).
58. L. Monin *et al*., γδ T cells compose a developmentally regulated intrauterine population and protect against vaginal candidiasis. *Mucosal Immunol.*, 10.1038/s41385-020-0305-7 (2020).
59. A. Wilharm *et al*., Mutual interplay between IL-17-producing γδT cells and microbiota orchestrates oral mucosal homeostasis. *Proc. Natl. Acad. Sci. U.S.A.* **116**, 2652–2661 (2019).
60. S. Krishnan *et al*., Amphiregulin-producing γδ T cells are vital for safeguarding oral barrier immune homeostasis. *Proc. Natl. Acad. Sci. U.S.A.* **115**, 10738–10743 (2018).

61. A. Bandeira *et al*., Localization of gamma/delta T cells to the intestinal epithelium is independent of normal microbial colonization. *J. Exp. Med.* **172**, 239–244 (1990).
62. A. S. Ismail, C. L. Behrendt, L. V. Hooper, Reciprocal interactions between commensal bacteria and gamma delta intraepithelial lymphocytes during mucosal injury. *J. Immunol.* **182**, 3047–3054 (2009).
63. V. Pitard *et al*., Long-term expansion of effector/memory Vdelta2-gammadelta T cells is a specific blood signature of CMV infection. *Blood* **112**, 1317–1324 (2008).
64. L. De Bolle, L. Naesens, E. De Clercq, Update on human herpesvirus 6 biology, clinical features, and therapy. *Clin. Microbiol. Rev.* **18**, 217–245 (2005).
65. L. Hviid *et al*., High frequency of circulating gamma delta T cells with dominance of the v(delta)1 subset in a healthy population. *Int. Immunol.* **12**, 797–805 (2000).
66. M. Lawand, J. Déchanet-Merville, M.-C. Dieu-Nosjean, Key features of gamma-delta T-cell subsets in human diseases and their immunotherapeutic implications. *Front. Immunol.* **8**, 761 (2017).
67. F. Jouen-Beades *et al*., Expansion of circulating V gamma 9/V delta 1 T cells in a patient with a syndrome of recurrent fever: Evidence for an unusual antigen-driven process leading to selection of recurrent motifs within TCR junctional loops of diverse lengths. *Eur. J. Immunol.* **29**, 3338–3349 (1999).
68. J. Marißen *et al*., Efficacy of Bifidobacterium longum, B. infantis and Lactobacillus acidophilus probiotics to prevent gut dysbiosis in preterm infants of 28+0-32+6 weeks of gestation: A randomised, placebo-controlled, double-blind, multicentre trial: The PRIMAL clinical study protocol. *BMJ Open* **9**, e032617 (2019).
69. D. A. Bolotin *et al*., MiXCR: Software for comprehensive adaptive immunity profiling. *Nat. Methods* **12**, 380–381 (2015).
70. M. Shugay *et al*., VDJtools: Unifying post-analysis of T cell receptor repertoires. *PLOS Comput. Biol.* **11**, e1004503 (2015).
71. V. I. Nazarov *et al*., tcR: An R package for T cell receptor repertoire advanced data analysis. *BMC Bioinformatics* **16**, 175 (2015).